Effects of multi-walled carbon nanotubes on metal transformation and natural organic matters in riverine sediment

Piao Xu [a,b], Ming Chen [a,b], Guangming Zeng [a,b,*], Danlian Huang [a,b,*], Cui Lai [a,b], Ziwei Wang [a,b], Ming Yan [a,b], Zhenzhen Huang [a,b], Xiaomin Gong [a,b], Biao Song [a,b], Tao Li [a,b], Abing Duan [a,b]

[a] College of Environmental Science and Engineering, Hunan University, Changsha 410082, P.R. China.

[b] Key Laboratory of Environmental Biology and Pollution Control, Ministry of Education, Hunan University, Changsha 410082, P.R. China.

[*] Corresponding Authors

E-mail: zgming@hnu.edu.cn (Guangming Zeng). Fax: +86-731-88823701; Tel: +86-73- 88823701.

E-mail: huangdanlian@hnu.edu.cn (Danlian Huang).

Abstract

In this study, pragmatic prospection of multi-walled carbon nanotubes (MWCNTs) is conducted considering their impacts on Cd transformation, microbial activity and natural organic matter (NOM) in sediments. Indeed, dose-dependent of MWCNTs acceleration in Cd sedimentation and immobilization in water-sediment interface has been found. Unexpectedly, even with the reduced Cd bioavailability, high ratios of MWCNTs incorporation led to exacerbated microbial inactivation. Besides, we noted that MWCNTs significantly lowered NOM contents in sediments. Chemical characterization results also demonstrated that high ratios of MWCNTs incorporation reduced the aromaticity, hydrophobicity and humification of fulvic acid (FA) and humic acid (HA) in sediments. The Cd binding results confirmed that quantity and chemical variation of NOM affected their central ability to Cd binding, referring to significant decrease in combined Cd contents. The findings indicated that reduction in humic substances and chemical structure variation might be the important reason attributed to the MWCNTs toxicity. This study provides novel mechanisms understanding the fate of carbon nanotubes considering the balance in environmental benefit and potential risks.

Keywords: Natural organic matter; Multi-walled carbon nanotubes; Humic substances; Metal; Environmental risk.

1. Introduction

The production and use of carbon nanotubes (CNTs) have rapidly increased [1-4]. Annual global production of CNTs has reached several thousand metrictons. According to a market research report, production capacity of CNTs products was about 4, 065 tons in 2010 and 12, 300 tons in 2015 [5]. The increasing production and application of CNTs will inevitably lead to their accumulation in environment. Environmental modeling predicts that soils and sediments tend to be the primary sites for inorganic metals, metalloids and organic chemicals, and also for engineered nanomaterials (ENMs) [6-8]. Once accumulated in soils/sediments, CNTs might interact with chemical contaminants, microbes, minerals and organic matter [9]. Actually, considerable attention has been focused on their interactions between pollutants co-existed in environment. Recently, Sun et al. [10] reported that CNTs amendment increased Cd adsorption capacity at CNTs/sediments ratios ranging from 1.25% to 10%. In our previous study [11], we also found that MWCNTs (0.5%-1.5%) could distinctly decrease the aqueous concentrations of phenanthrene and Cd released from the sediments. Indeed, CNTs could affect the pollutants transformation in environment.

Thus far, widely varying impacts (both positive and negative) of CNTs have been reported, possibly owing to their environmental application of CNTs as adsorbents or membranes [12, 13] and also their inherent cytotoxicity and antimicrobial activity [14]. CNTs applied and enriched in environment affected bioavailability and toxicity of contaminants in various pathways [2, 12]. For example, Yu and Wang [15] found that raw CNTs significantly reduced Zn and Cd uptake rate, possibly due to their effects on

the physiological activity of *Daphnia magna*. Meanwhile, microbial inactivation is an important theoretical pre-testing indicator of environmental impact [14]. Studies suggested that both MWCNTs and SWCNTs could lower microbial activity and microbial biomass. Thus, even taking advantages of environmental benefit in promoted contaminants transport, pragmatic prospection and cautious consideration of CNTs are considerable since their intrinsic toxicity and ecological threats.

Actually, impact of CNTs is a complex function of nanomaterial physicochemical property, transport behavior and environment chemistry. Recently, Tong et al. [16] reported that SWCNTs were toxic to soil bacteria, caused minor shifts in microbial community and brought about negatively effects on metabolic function. They also hypothesized that natural organic matter (NOM) tended to be a primary factor ascribed to microbial toxicity, since the retention of chemicals by soil organic matter. Accordingly, NOM is ubiquitous in the environment and is composed of a complex mixture of polyelectrolytic and organic molecules that varied spatially and temporally in molecular composition, acidity and charge density [17, 18]. It has been well known that NOM could interact with chemical contaminants (such as metals and organic pollutants) and surfaces of ENMs. Generally, NOM can increase the stability of ENMs by surface attaching donating with electrostatic repulsion [19, 20], and destabilize through charge neutralization, bridging [21], and pearls-on-a-string formation [22]. Such interactions might affect the fate of ENMs in realistic conditions. For example, humic acids (HA) lowered the LC_{50} of $nTiO_2$ to zebrafish from 290 mg/L to 156 mg/L via increasing the TiO_2 NPs suspension stability [23]. According to Zhang et al. [24],

the presence of HA alleviated the nanotoxicity of MWCNTs to alga because of the depressed oxidative stress and the inhibited cell penetration and internalization. Hyung et al. [25] also reported an enhanced stabilizing propensity of MWCNTs in the presence of aromatic fractions of NOM in the aqueous phases.

Given the potential for metal immobilization and inherent interactions between CNTs and NOM, there is a need to understand interactions among CNTs, metals and NOM. Yet scarce study focused on the fate of CNTs systematic considering the interactions among MWCNTs, chemical contaminants and NOM ubiquitous in natural environment. Thus, the present study aims to facilitate a better understanding of the fate of CNTs in natural environment. Cd is selected as representative contaminant because of their large-scale contamination and serious toxicity [8]. MWCNTs are chosen due to their large application [2]. Meanwhile, wide range of MWCNTs ratios were incorporated in order to discuss the balance in environmental benefit and ecological risk of MWCNTs. The primary goals were to: (1) evaluate the potential roles of MWCNTs in Cd transport and passivation in water-sediment interface, (2) investigate the fate of MWCNTs by full considering the co-existing metals and NOM, and (3) explore the mechanisms of ecological risk of MWCNTs.

2. Materials and methods

2.1. Materials

Sediments were collected from the 5–15 cm layer from Xiangjiang River in Changsha, China. After air drying, sediment samples were grinded and sieved prior to the experiments. Chemicals used were analytical reagents of high purity. Ultrapure water

(resistivity >18.2 MΩ-cm) was used for the experiments. The sediment had a neutral pH (6.65) and an organic carbon content of 23.81 g/kg. MWCNTs were purchased from Chinese academy of sciences, Chengdu organic chemistry Co., Ltd. Accordingly, MWCNTs (TNM3, arraying with 10–20 nm diameter and 10–30 μm length) were synthesized by CVD method via natural gas catalytic decomposition over Ni-based catalyst and pretreated with HNO_3. The sample purity is >98% and ash (catalyst residue) <1.5%. MWCNTs were characterized by transmission electron microscopy (TEM, FEI Tecnai G2 F20), nitrogen adsorption–desorption Brunauer, Emmett and Teller (BET) measurements and X-ray photoelectron spectra (XPS) (Thermo ESCALAB 250XI, Thermo Scientific, USA). Point of zero charge (PZC) were estimated by determining the zeta potential according to the standard drift test method [26, 27].

2.2. Experiment setup

Considering the possible roles of MWCNTs in environmental application, relatively high ratios of MWCNTs were considered in this study. The collected sediments were mixed with certain amounts of MWCNTs to prepared MWCNTs-sediment mixture at certain mass proportions of 0% (B), 0.1% (C), 1% (D), 2.5% (E) and 5% (F). Blank control was set as ultrapure water-sediment mixture (A). The prepared MWCNTs-sediment mixture was vibrated at 30 rpm for 72 h. 50 g of MWCNTs-sediment mixture was settled to a serum bottle, and then 500 mL Cd-containing solution (50 mg/L, pH 6.0) was added gently. Considering the reality of possible high levels of Cd in sediments along Xiangjiang river, relatively high Cd concentration was used in our study. The samples were stewing for 10, 30, 60 and 90

days, respectively. Each sample was performed at least in triplicate and results were presented as the average and standard deviation of the replicates. MWCNTs were collected via ultrasonic, suspension and separation procedures for several times to separate from sediments at day 90, due to the lightweight and surface hydrophobicity of MWCNTs. The collected MWCNTs were characterized by TEM and XPS. In order to investigate the potential adsorption ability of NOM by MWCNTs, the adsorption experiments were conducted with the extracted FA/HA fractions (TOC, 50 mg/L) at the presence of 1 g/L MWCNTs at neutral pH according to Hyung and Kim [28].

2.3. Cd analysis

The supernatant in the prepared samples was filtered through 0.45 μm membrane for the Cd testing in order to investigate Cd sink in the experimental systems. Metal speciation (classified as exchangeable fraction (F1), reducible fraction (F2), oxidizable fraction (F3) and residual fraction (F4)) was detected by modified BCR procedure [29]. Briefly, 0.50 g of the dry samples was sequentially extracted by four steps (Supporting information (SI), Table S1). Each of the extracted solutions was filtered (0.45 μm membrane) and diluted for Cd analysis. Cd risk assessment and bioavailability was evaluated using the toxicity characteristic leaching procedure (TCLP) according to Wan et al. [29]. Cd concentration was determined by atomic absorption spectrophotometer (AAS, Agilent 3510, USA).

2.4. Humic substances extraction and fractionation

The humic components were extracted according to methods recommended by the international humic substances society (IHSS) [30] with minor modifications. 2.0 g

sediment was pretreated with 1.0 M HCl (pH 1.0-2.0) for three times. The pH of treated sediment was then adjusted to 7.0. For humic substance extraction, 15 mL of $NaOH/Na_2P_2O_7$ mixture (1.0 M, pH 13.0) was added and shake for 1 h at 70 ℃, and then collected by centrifugation and filtration. The extraction procedure was repeated for four times. The extract was collected and diluted to 100 mL to obtain the HS contents. The extraction efficiency for HS was above 95% in all samples. For HA and FA extraction, 25 mL of HS solution was employed and treated with 1.0 M H_2SO_4 to adjust the pH to 1.0, preserved at 60 ℃ for 1 h, and then rest overnight for the complete precipitation of HA. Separation of HA and FA was further conducted via centrifugation (5000 rpm, 15 min) and filtration repeated for three times. Total organic carbon of humic substances (HS, HA and FA) were analyzed via TOC analyzer. Besides, the extracts of HS and FA was further digested by HNO_3 solution (1:1, v/v) via the microwave digestion instrument to investigate the HS/FA combined Cd by AAS.

2.5. Chemical structure analysis of humic substances

The pre-filtered HA and FA samples at day 10 and 60 were diluted to a TOC level of approximately at 15 ± 0.5 mg/L using ultrapure water. A fluorescence spectrometer (F7000, Hitachi, Japan) was employed to obtain the three-dimensional excitation-emission matrix (3DEEM) spectra of the HA and FA. The samples were scanned over excitation wavelengths between 220-400 nm (5 nm bandwidth) and emission wavelengths between 250-600 nm (5 nm bandwidth). An EEM of the ultrapure water was obtained and subtracted from the EEM of each sample in order to remove most of the Raman scatter peaks. FA fraction was further freeze dried and collected for Fourier

transform infrared spectrophotometer (FTIR) analysis (Nicolet, Nexus-670). Meanwhile, we also measured the UV-vis spectra and specific UV absorbance (SUVA) at the TOC value of 15 ± 0.5 mg/L.

2.7. Statistical analysis

The results were presented as the means and the standard deviations of three replicates. The differences between the means were analyzed by one-way analysis of variance (ANOVA) and differences at $p < 0.05$ were considered as significant. To compare the response of microbial activity of the tested sediments, a dimensionless parameter, enzyme activity change response (ACR), was introduced.

$$ACR=(A_{sample} - A_{control})/A_{control}$$

$A_{control}$ and A_{sample} denoted enzyme activity of control and Cd/MWCNTs amended sediments, respectively. ACR depicted the relative toxicity level of the chemical incorporation to enzyme activity in sediments.

3. Results and discussion

3.1. Characterization of MWCNTs and sediments

The initial HS content in Xiangjiang riverine sediment was 6761.25 mg/kg (SI, Fig. S1). Considering the possible effect of MWCNTs on HS extraction, HS contents in sediments with 1% and 2.5% MWCNTs were detected and calculated at the value of 6831.12 and 6717.75 mg/kg, respectively. Results demonstrated that no significant (p>0.05) difference was observed, suggesting that the adopted method was available for complete HS extraction.

PZC of MWCNTs was measure at 6.4 (SI, Fig. S2), which is around the solution pH 6.0), suggesting the weak electrostatic interaction between Cd and MWCNTs. Fig. 1 shows the representative TEM images of pristine MWCNTs (a) and TEM images of sediment after incubated with MWCNTs for 90 days (b, c). The MWCNTs had smooth surfaces and cylindrical shapes with 10–20 nm outer diameter. The specific surface area of the MWCNTs was 211.428 m^2/g and the main pore inner diameter was 3.03 nm according to N_2 adsorption–desorption isotherms. The relatively high surface area was beneficial to metal adsorption. MWCNTs were uniformly dispersed and interspersed with sediments. From Fig. 1(b-c), no significant aggregation and variation was found for MWCNTs after 90 days of incubation. XPS data provide information on the graphitic order of the CNTs and the chemical nature of the functional groups through analysis of the C1s and O1s XP spectra. As shown in Fig. 1e, the C1s core level peak position of the carbon atoms was approximately at 283.5 eV with no significant variation. The pristine MWCNTs at day 0 showed traces of nitrogen (1.12%) and oxygen (3.06%), and no Cd was found (<0.01%). The peak position for oxygen was centered at 531.79 eV and 532.89 eV in MWCNTs at day 0 and day 90, respectively. The apparent binding energy of the main peak differed slightly between two samples. At day 90, the content of C and N was decreased to the percent of 91.7% and 0.94%, respectively, while the O content increased to 6.29%.

To highlight the change in the distribution of C and O species, C1s and O1s XP spectra has been analyzed. According to the difference spectra analysis method, four components were present in the C1s spectrum. The following bonds were assigned: sp^2

C=C (C1, 284.67 and 284.59 eV), sp^3 C–C (C2, 285.10 and 284.99 eV), C–O (C3, 286.1 and 285.88 eV) and (C4, 290.61 and 289.96 eV) [31]. Results demonstrated that MWCNTs were relatively stable, which were consistent with previous studies that CNTs were some of the most refractory synthetic nanomaterials [32]. For O1s analysis, the bonds assigned C=O (O1, 531.01 and 530.68 eV), O=C-O (O2, 532.18 and 532.20 eV) and C-OH (O3, 533.24 and 533.90 eV). Commonly, a slight change in binding energy <0.35eV is considered insignificant based on the energy resolution of the XPS instrument used. As shown in Fig. 1g, significant chemical shifts and peak values variation were observed in C-OH and -O-C=O, possible reason might be the interactions between MWCNTs and organic matters in sediments. Numerous studies have confirmed that the hydrophobic parts and aromatic monomers of NOM, including carboxyl, carbonyl, hydroxyl and phenolic groups, had strong affinity to CNTs through hydrophobic and π–π interactions [17, 33]. In our study, we investigated that the adsorption capacity of FA and HA was 6.96 mg/g and 10.21 mg/g of the tested MWCNTs, respectively. Thus, potential adsorption of NOM might contribute to the variations of C-OH and -O-C=O of MWCNTs. However, studies were conducted in aquatic environment, detail research will be given to address the underlying interactions between MWCNTs and NOM.

3.2. Effect of MWCNTs on Cd immobilization and bioavailability

Residual Cd concentrations in the aqueous supernatant are shown in Fig. 2. Results showed the rapid sink of aqueous Cd to sediment. Almost 80% of Cd sedimentation occurred in natural sediment at day 10, while higher than 85% deposited in sediment

with MWCNTs incorporation. At day 60, residual Cd concentrations were all below 0.1 mg/L in all tested samples. The potential sink of the heavy metals corresponded to the strong affinity of sediment, usually dominated by particle adsorption and complexation to various compartments in natural sediment [34]. MWCNTs incorporation promoted Cd sedimentation, mainly due to the binding affinity of MWCNTs [33].

Commonly, metals accumulated in sediment are bound as diverse forms, such as occluded in amorphous materials, adsorbed on clay surfaces, complexed with natural organic matter, immobilized in lattice of primary minerals and secondary minerals [34, 35]. Of the tested four fractions, exchangeable fraction (F1) and reducible fraction (F2) were presented at the highest concentrations (SI, Fig. S3). Elevated levels of oxidizable fraction (F3) and residual fraction (F4) occurred on account of the adsorption and immobilization ability of sediments. Apparently, high levels of MWCNTs promoted Cd transformation in sediments. For example, the decrease of F1 contents from 263.62 mg/kg to 190.96 mg/kg was observed in samples with 5.0% MWCNTs from day 10 to day 90, while the F1 contents varied gradually from 239.68 mg/kg to 203.68 mg/kg in samples without MWCNTs (SI, Table S2). Results demonstrated that MWCNTs promoted Cd immobilization in riverine sediments. Moreover, high ratios of MWCNTs were more benefit to Cd sedimentation and immobilization.

Generally, the TCLP-extractable metal is called the bio-accessible pool. The TCLP extracted Cd contents in all the samples exceeded the USEPA hazardous waste criteria of 5 mg/kg, ranging from 170.08 mg/kg to 332.64 mg/kg (Fig. 2). The highest bio-accessible Cd concentration was found at samples without MWCNTs. Significant

depletion in TCLP Cd contents was obtained in sediment with MWCNTs. At day 90, TCLP extracted Cd concentration was 329.2, 305.9, 223.2, 192.6 and 175.8 mg/kg in MWCNTs-incorporated sediment with the ratios at 0%, 0.1%, 1%, 2.5% and 5%, respectively. The results demonstrated that MWCNTs accelerated Cd sedimentation and lowered Cd bioavailability. Benefiting from the admirable binding ability to metals and metalloids, metal adsorption by MWCNTs is an important fate controlling metal bioavailability in aquatic environment.

3.3. Effect of Cd and MWCNTs on microbial activity

The assessment of sediment enzyme activities could serve as indicator regarding variations in metal bioavailability, organic matter and nutrient cycling in sediments. Accordingly, toxic chemical exposure commonly decreases microbial biomass/activity, affects key microbial process and even changes the functional diversity of microbial communities [36, 37]. Data in Fig. S4 demonstrated the urease and catalase variation for up to 90 days. Microbial activity was strongly influenced by the Cd and MWCNTs. Reduction in enzyme activity exposed to toxic Cd was observed. Initially, lower ratios of MWCNTs incorporation remitted the sharp reduction in urease and catalase activities. However, after 60 days of incubation, even more remarkable inhibition occurred with the MWCNTs co-incorporation, especially in the groups with high ratios of MWCNTs. Possible reason might be the intrinsic toxicity of MWCNTs to microbes, which agreed with previous studies suggesting that carbon nanomaterials induced some level of toxic response, such as growth inhibition and antimicrobial activity [38].

Indeed, MWCNTs promoted Cd sedimentation in a concentration-dependent fashion on account of the Cd adsorption ability of MWCNTs. However, we noted that MWCNTs inhibited the urease activities with the activity change response (ACR) below 1.0 in the all tested samples (Fig. 3a), and also lower than samples without Cd. At day 10, the ACR was calculated at the value of 0.795 and 0.833 in the sample with 2.5% MWCNTs incorporation with and without Cd, respectively. Moreover, ACR was observed ranging from 0.971 to 0.833 exposed to 0.1% and 2.5% MWCNTs without Cd respectively, declaring the inherent toxicity of MWCNTs. Results were coordinated with previous study which reported that acute toxicity aggravated factually with the addition of nanomaterials, although metal bioaccumulation and bioavailability decreased [39, 40]. Wang et al. [41] reported that CNTs and metals transiently affected microbial communities, and co-existence of CNTs and metals intensified the microbial toxicity. Possible reason might be that the destruction of cell walls by CNTs brought about the accessible microbial bioaccumulation of heavy metals [42-44]. In conclusion, results demonstrated that even with the positive role of alleviation of Cd bioavailability via acceleration of Cd transformation, severe toxicity occurred with coexisting of Cd and MWCNTs.

3.4. Effect of Cd and MWCNTs on humic substances quantity

Laboratory and field studies have reported that humus is one of most important NOM sources in soils and sediments [45, 46]. In our study, we noted that a gradual decrease in HS and HA carbon occurred from day 10 to day 90 (Fig. 4), while no significant variation occurred in FA. In comparison with Cd contaminated samples,

MWCNTs addition largely reduced the extractable HS and HA carbon. For example, HS carbon was highest in control (6320.83 mg/kg) followed by Cd amended sample (6182.92 mg/kg), and then followed by a large decrease in Cd and MWCNTs co-amended samples, such as sample with 0.1% MWCNTs (5955.83 mg/kg) and 2.5% MWCNTs (4748.52 mg/kg) at day 30. Particularly, a significant MWCNTs based dose-dependent decrease in HS contents was observed during the whole 90 days. Significant HA reduction occurred during the initial 30 days compared to controls without Cd sink ($p < 0.01$). Peak values of FA contents in control sediment reached 4289.33 mg/kg at day 30, and then a gradual decrease occurred. HA contents were quite lower than FA contents in the tested sediments. Unlike HA, no obvious difference was found in FA with low ratios of MWCNTs (<2.5%).

The wide range of the HS indicated the distinct impact of MWCNTs on humic substances in sediments. Accordingly, humus is the product of a series of biological activity. Humus transformation is interrelated to microbial activity [47]. Cd and MWCNTs are acknowledged as toxic chemicals and are recognized to reduce microbial activity, thus extraneous Cd and MWCNTs contamination resulted in the alleviation of HS reduction. Additionally, another possible reason might be the adsorption of HS on MWCNTs. Previous studies have demonstrated that HS fractions, particularly HS fraction with hydrophobic and/or lower molecular weight, could adsorb on the MWCNTs [48]. In our study, the adsorption capacity of FA and HA was 6.96 mg/g and 10.21 mg/g of the tested MWCNTs, respectively. Thus, we suggested that adsorption of FA and HA could be negligible in the case of the significant differences. Accordingly,

further investigation focused on FA and HA chemical structure was conducted in the current study.

3.5. Effect of Cd and MWCNTs on chemical structure of humic substances

Excitation-emission matrices (EEM) are used to visually illustrate the changes in chemical structure of FA and HA at day 10 and 60 (Fig. 5 and Fig. S5). Apparently, FA fraction yielded two peaks with fluorescence maximum at E_x/E_m around 315/430 nm (peak A) and 270/460 nm (peak B), which were operationally attributable to terrestrial humic-like components [49]. HA fractions existed three peaks at E_x/E_m around 230/320 nm (peak A), 270/330 nm (peak B) and 220/420 nm (peak C), respectively. The peak A and B were indicative of protein-like component, likely attributable to the activity of bacteria or plankton [49, 50]. Peak C around 230/420 nm was reported to be operationally attributable to the marine and terrestrial humic substances [51].

For brevity, EEM spectra at day 10 are detailed in the Fig. S5. An overall similarity was observed in 3D-EEM plots of FA at day 10 except for sample with 2.5% MWCNTs (SI, Fig. S5), suggesting an ignorable effect on FA initially with low levels of MWCNTs. However, obvious change was observed in 3DEEM plots of HA at day 60, especially in sample with 2.5% MWCNTs (Fig. 5). A distinct blue shift in E_m (25 nm) of FA was found between control and sample with 2.5% MWCNTs at day 60 (Fig. 5 and Table S3). It was also interesting to note that peaks of HA varied significantly in the tested samples. The E_x/E_m of Peak A in control occurred at 275/335 shifted to 270/330 nm in the sample with 2.5% MWCNTs (SI, Table S4). Generally, a blue shift in E_m was caused by a structural change resulting from two possible pathways: (i) reduction in the extent

of the π-electron system, rising from a reduction in aromatic rings or conjugated bonds in a chain structure, or conversion of a linear ring system to a non-linear system; (ii) reduction of certain functional groups, for instance, hydroxyl, carbonyl and amine [52].

Meanwhile, fluorescence intensity (FI) levels at peak A decreased markedly with Cd exposure both in FA and HA (SI, Table S3-S4). Results were accordant with the previous studies which reported that the fluorescence quenching curve of the humic-like components showed good relationship with the heavy metals level, such as with Hg(II) [53, 54], Cu(II) [55] and Pb(II) [56] etc. In addition, the max FI levels of HA/FA fractions decreased significantly with MWCNTs incorporation, implying that high levels of MWNCTs affected the HA/FA structure markedly. For example, MWCNTs caused larger quenching effect of HA at peak A with 0.1% MWCNTs (11.21%) and 2.5% MWCNTs (36.82%) at day 60. The FI may be reduced in two ways: (i) removal of fluorescent compounds by formation of metal-NOM complexation; (ii) damage of fluorescent compounds by MWCNTs.

Results of UV absorbance data for FA fractions were shown in Fig. 6 and Fig. S6. The FA fractions in control samples were much more aromatic and humified (noted as a highest A_{254} and A_{280}), and of higher hydrophobicity (noted as a highest A_{260}). Accordingly, absorbance at 254 nm (A_{254}) and 260 nm (A_{260}) is reported to positively interrelated to humification and hydrophobicity, respectively [57-59]. Meanwhile, A_{280} (absorbance at 280 nm) is positively correlated to aromaticity, whereas E_2/E_3 (absorbance at 250 nm divided by that at 365 nm) and $f_{450/500}$ (fluorescence intensity at E_m 450 nm divided by that at 500 nm at E_x 370 nm) are negatively correlated to

aromaticity [19]. In samples with 2.5% MWCNTs, we observed a significant reduction in the specific absorbance at A_{254}, A_{260} and A_{280}. The lower values of A_{260} indicated the lower hydrophobic content in FA fractions, and then inhibited the possible activity of pollutant migration and transformation. In addition, the lowest A_{254} value was observed in sample with 2.5% MWCNTs, indicating that MWCNTs incorporated samples were richer in unsaturated carbon bonds compared to other samples. Apparently, high MWCNTs (2.5%) inhibited the aromaticity and hydrophobicity of FA remarkedly with significant higher $f_{450/500}$ and E_2/E_3. Results were quite agreed with the 3DEEM and TOC results of FA.

To better understand the chemical structure of HA fractions, FTIR analysis was conducted (Fig. 7). A strong hydrogen bonded (O–H) stretching transmission occurred around 3400 cm^{-1} and a prominent C–H stretching transmission was found around 2920 cm^{-1} [60, 61]. The peaks intensity around 1640 cm^{-1} represented carbonyl (–C=O) stretching [62], while peaks around 1240 cm^{-1} were assigned as for syringyl ring and C–O stretch in humic acids [63]. The relative variation in the band intensity corresponded to the difference in the level of respective functional groups. Obviously, Cd incorporation sample showed a decrease at 3402, 2921, 1643 and 1238 cm^{-1} compared to control. While samples incorporated with 0.1% MWCNTs showed no significant difference compared with control sample. In the case of sample with 2.5% MWCNTs, the intensities of hydrogen bands at 3398 cm^{-1}, C–H stretching at 2920 cm^{-1} and carbonyl bands at 1637 cm^{-1} decreased. Results suggested a richness of humic structures in control sample and a loss of readily available aliphatic compounds in

MWCNTs incorporated samples. Therefore, these observed correlations collectively suggested that high levels of MWCNTs exposure led to destruction of their chemical structures and thus lead to the HS deterioration, possibly via reducing the functional groups and/or aromatic rings.

3.6. Effect of MWCNTs on Cd complexation ability of humic substances

We noted that MWCNTs induced HA and FA structural variation, with inhibiting of their aromaticity, hydrophobicity and humification. Accordingly, the aromaticity of NOM is correlated to an increased binding capacity of metal ions [64]. Numerous studies confirmed that HS were dominated in controlling the speciation, fate, transport, bioavailability and toxicity of certain metal ions in nature environment through various metal binding reactions [65]. Obviously, Cd and MWCNTs incorporation significantly affected the Cd contents bond with HS and FA (Fig. 8). HS bond Cd amount was varied from 2.80 to 35.75 mg/kg sediment and FA bond Cd was ranged from 1.62 to 19.72 mg/kg sediment. Compared to the single Cd exposure, MWCNTs incorporation significant depleted the combined Cd contents. FA is a highly oxidized, biologically stable, water-soluble naturally occurring complexing agent that can complex metal ions [66]. Previous studies demonstrated Cd commonly bond by the outer-sphere mechanism, associated with the metal binding affinity of quinone carbonyl groups in FA [67]. In our present study, exogenous FA addition also promoted Cd transformation and immobilization in sediments (SI, Fig. S7).

Besides, mass ratios of Cd combined by HS and FA were further calculated as per unit of humic substance mass (expressed as TOC) (Fig. 8). It was apparent that

MWCNTs reduced the Cd binding contents in unit mass of HS and FA (p<0.01). For example, FA bond Cd amount decreased from 3.83 to 2.98 mg/g FA (TOC) in 0% and 2.5% MWCNTs incorporated sample at day 90, respectively. Results suggested that MWCNTs affected the Cd complexation ability in sediments on account of the mutual interactions among heavy metals, humic substances and MWCNTs. On the one hand, HS contain numerous potential binding sites for metal ions, such as carboxylic, phenol, hydroxyl, amine, and quinone groups. On the other hand, HA and FA could bind to CNTs through strong π-π interactions, which might affect the adsorption of heavy metals on both HS and CNTs [25]. For instance, Lan et al. [68] reported that the activation free energy was increased from 18.3 in HA-uranyl binary system to 20.0 kJ/mol with CNTs, suggested that the hydrated uranyl structure may be stabilized in the presence of CNTs. This result could be applicable to previously studies which reported the humic substances as mainly metal binding material in sediments, participating in metal distribution and transformation [69]. In general, this study demonstrated that high ratios of MWCNTs incorporation led to reduction in NOM levels certainly accompanied with the decrease in humic bond Cd. The study suggests that dose-dependent response needs to be taken into account while evaluating the environmental application, considering the balance in environmental benefit (such as acceleration in immobilization and reduction bioavailability) and ecological risk (the potential toxicity of MWCNTs).

4. Conclusion

This study provided information about the effects of MWCNTs on metal

transformation, microbial activity and NOM in nature sediment. Our results revealed that once discharged into environment, MWCNTs promoted Cd sedimentation and immobilization, and reduced TCLP extracted Cd contents. However, no significant enhancement of microbial activity occurred even with the low Cd bioavailability. Further studies demonstrated that MWCNTs significantly impeded the quantity of NOM and altered their aromaticity, hydrophobicity and humification. In addition, quantity and chemical variation of HS significantly inhibited the metal complexation ability of HS, as we can observe significant decrease in HS complexed Cd amounts. The observed results indicated that MWCNTs incorporation was a key factor in determining the NOM in sediment, controlling NOM quantity, chemical structure and metal complexation ability as well, which might act as a facile indicator for risk assessment of MWCNTs. This study provides new insights on the mechanisms underlying the potential toxicity and ecological risk of carbon nanotubes.

ACKNOWLEDGMENTS

This study was financially supported by the Program for the National Natural Science Foundation of China (51709101, 51879101, 51609023, 51579098, 51779090, 51709101, 51521006), the National Program for Support of Top–Notch Young Professionals of China (2014), the Program for Changjiang Scholars and Innovative Research Team in University (IRT-13R17), and Hunan Provincial Science and Technology Plan Project (2018SK20410, 2017SK2243, 2016RS3026), and the Fundamental Research Funds for the Central Universities (531118010226, 531119200086, 531118010114, 531107050978).

Appendix A. Supplementary data

Additional MWCNTs and NOM characterization and microbial activity response were provided in the supporting information. Content includes Figures S1-S7 and Tables S1-S4.

References

[1] B. Song, P. Xu, G. M. Zeng, J. L. Gong, P. Zhang, H. P. Feng, Y. Liu, X. Y. Ren. Carbon nanotube-based environmental technologies: the adopted properties, primary mechanisms, and challenges, Rev. Envion. Sci. Bio/Technol. 17 (2018) 571-590.

[2] K. Goh, H. E. Karahan, L. Wei, T. H. Bae, A. G. Fane, R. Wang, Y. Chen, Carbon nanomaterials for advancing separation membranes: A strategic perspective, Carbon 109 (2016) 694-710.

[3] M. Chen, X. S. Qin, G. M. Zeng, Biodegradation of carbon nanotubes, graphene and their derivatives, Trend. Biotechnol. 35 **(**2017) 836-846.

[4] R. Q. Wang, L. J. Xie, S. Hameed, C. Wang, Y. Ying, Mechanisms and applications of carbon nanotubes in terahertz devices: A review, Carbon, 132 (2018) 42-58.

[5] A. Parish, Production and applications of carbon nanotubes, carbon nanofibers, fullerenes, graphene and nanodiamonds: A global technology survey and market analysis, *Stamford, CT, USA: Innovative Research and Products*, (2011).

[6] W. J. Xue, D.L. Huang,G. M. Zeng, J. Wan Jia, C. Zhang, R. Xu, M. Cheng, R. Deng. Nanoscale zero-valent iron coated with rhamnolipid as an effective stabilizer for immobilization of Cd and Pb in river sediments. J. Hazard. Mater. 341 (2018) 381-

389.

[7] P. Xu, G. M. Zeng, D. L. Huang, M. Yan, M. Chen, C. Lai, H. Jiang, H. P. Wu, G. M. Chen, J. Wan, Fabrication of reduced glutathione functionalized iron oxide nanoparticles for magnetic removal of Pb (II) from wastewater, J. Taiwan Inst. Chem. Eng. 71 (2017) 165-173.

[8] P. Xu, C. Lai, G. M. Zeng, D. L. Huang, M. Chen, B. Song, X. Peng, J. Wan, L. Hu, A. B. Duan, W. W. Tang, Enhanced bioremediation of 4-nonylphenol and cadmium co-contaminated sediment by composting with *Phanerochaete chrysosporium* inocula, Bioresour. Technol. 250 (2018) 625-634.

[9] Y. Wang, C. H. Chang, Z. Ji, D. C. Bouchard, E. M. Nisbet, J. P. Schimel, J. L. Gardea-Torresdey, P. A. Holden, Agglomeration determines effects of carbonaceous nanomaterials on *Soybean Nodulation*, dinitrogen fixation potential, and growth in soil, ACS Nano, 11 (2017) 5753-5765.

[10] W. Sun, B. Jiang, F. Wang, N. Xu, Effect of carbon nanotubes on Cd(II) adsorption by sediments, Chem. Eng. J. 2654 (2015) 645-653.

[11] B. Song, G. M. Zeng, J. L. Gong, P. Zhang, J. Q. Deng, C.H. Deng, J. Yan, P. Xu, C. Lai, C. Zhang, M. Cheng. Effect of multi-walled carbon nanotubes on phytotoxicity of sediments contaminated by phenanthrene and cadmium, Chemosphere 172 (2017) 449-458.

[12] S. Kabiri, D. N. H. Tran, T. A. Altalhi, D. Losic, Outstanding adsorption performance of graphene–carbon nanotube aerogels for continuous oil removal, Carbon, 80 (2014) 523-533.

[13] B. Song, P. Xu, G. Zeng, J. L. Gong, X. Wang, J. Yan, S. Wang, P. Zhang, W. Cao, S. Ye, Modeling the transport of sodium dodecyl benzene sulfonate in riverine sediment in the presence of multi-walled carbon nanotubes, Water Res. 129 (2018) 20-28.

[14] C. D. Vecitis, K. R. Zodrow, S. Kang, M. Elimelech, Electronic-structure-dependent bacterial cytotoxicity of single-walled carbon nanotubes, ACS Nano 4 (2010) 5471-5479.

[15] Z. G. Yu, W. X. Wang, Influences of ambient carbon nanotubes on toxic metals accumulation in *Daphnia magna*, Water Res. 47 (2013) 4179-4187.

[16] Z. Tong, M. Bischoff, L. F. Nies, P. Myer, B. Applegate, R. F. Turco, Response of soil microorganisms to as-produced and functionalized single-wall carbon nanotubes (SWNTs), Environ. Sci. Technol. 46 (2012) 13471-13479.

[17] D. H. Lin, X. L. Tian, T. T. Li, Z. Y. Zhang, X. He, B. S. Xing. Surface-bound humic acid increased Pb^{2+} sorption on carbon nanotubes, Environ. Pollut. 167 (2012) 138-147.

[18] A. M. Vindedahl, J. H. Strehlau, W. A. Arnold, R. L. Penn, Organic matter and iron oxide nanoparticles: aggregation, interactions, and reactivity, Environ. Sci.: Nano, 2016, **3**, 494-505.

[19] Y. P. Chin, G. Aiken, E. Oloughlin, Molecular weight, polydispersity, and spectroscopic properties of aquatic humic substances, Environ. Sci. Technol. 28 (1994) 1853-1858.

[20] S. M. Louie, E. R. Spielman-Sun, M. J. Small, R. D. Tilton, G. V. Lowry,

Correlation of the physicochemical properties of natural organic matter samples from different sources to their effects on gold nanoparticle aggregation in monovalent electrolyte, Environ. Sci. Technol. 49 (2015) 2188-2198.

[21] J. Buffle, K. J. Wilkinson, S. Stoll, M. Filella, J. Zhang, A generalized description of aquatic colloidal interactions: the three-colloidal component approach, Environ. Sci. Technol. 32 (1998), 2887-2899.

[22] P. H. Santschi, E. Balnois, K. J. Wilkinson, J. Zhang, J. Buffle, L. Guo, Fibrillar polysaccharides in marine macromolecular organic matter as imaged by atomic force microscopy and transmission electron microscopy, Limnol. Oceanogr. 43 (1998) 896-908.

[23] S. P. Yang, O. Bar-Ilan, R. E. Peterson, W. Heideman, R. J. Hamers, J. A. Pedersen, Influence of humic acid on titanium dioxide nanoparticle toxicity to developing zebrafish, Environ. Sci. Technol. 47 (2013) 4718-4725.

[24] L. Zhang, C. Lei, J. Chen, K. Yang, L. Zhu, D. Lin, Effect of natural and synthetic surface coatings on the toxicity of multiwalled carbon nanotubes toward green algae, Carbon, 83 (2015) 198-207.

[25] H. Hyung, J. D. Fortner, J. B. Hughes, J. H. Kim, Natural organic matter stabilizes carbon nanotubes in the aqueous phase, Environ. Sci. Technol. 41 (2007) 179-184.

[26] M. A. Kazakova, A. S. Andreev, A. G. Selyutin, A. V. Ishchenko, A. V. Shuvaev, V. L. Kuznetsov, O. B. Lapina, J. B. d'Espinose de Lacaillerie, Co metal nanoparticles deposition inside or outside multi-walled carbon nanotubes via facile support pretreatment. Appl. Surf. Sci. 456 (2018) 657-665.

[27] Annual Book of ASTM Standard, Standard test method for determination of contact pH with activated carbon, Philadelphia PA, United State of America, 2011.

[28] H. Hyung, J. H. Kim, Natural organic matter (NOM) adsorption to multi-walled carbon nanotubes: Effect of NOM characteristics and water quality parameters, Environ. Sci. Technol. 42 (2008) 4416–4421.

[29] J. Wan, C. Zhang, G. M. Zeng, D. L. Huang, L. Hu, C. Huang, H. P. Wu, L. L. Wang, Synthesis and evaluation of a new class of stabilized nano-chlorapatite for Pb immobilization in sediment, J. Hazard. Mater. 320 (2016) 278-288.

[30] S. Kuwatsuka, A. Watanabe, K. Itoh, S. Arai, Comparison of two methods of preparation of humic and fulvic acids, IHSS method and NAGOYA method, Soil Sci. Plant Nutr. 38 (1992) 23-30.

[31] T. I. T. Okpalugo, P. Papakonstantinou, H. Murphy, J. McLaughlin, N. M. D. Brown, High resolution XPS characterization of chemical functionalised MWCNTs and SWCNTs, Carbon, 43 (2005) 153–161.

[32] C. W. Lam, J. T. James, R. McCluskey, R. L. Hunter, Pulmonary toxicity of single-wall carbon nanotubes in mice 7 and 90 days after intratracheal instillation, Toxicol. Sci. 77 (2004) 126-134.

[33] W. W. Tang, G. M. Zeng, J. L. Gong, J. Liang, P. Xu, C. Zhang, B. B. Huang, Impact of humic/fulvic acid on the removal of heavy metals from aqueous solutions using nanomaterials: a review, Sci. Total Environ. 468 (2014) 1014-1027.

[34] C. Zhang, Z. G. Yu, G. M. Zeng, M. Jiang, Z. Z. Yang, F. Cui, M. Y. Zhu, L. Q. Shen, L. Hu, Effects of sediment geochemical properties on heavy metal

bioavailability, Environ. Inter. 73 (2014) 270-281.

[35] J. Liang, Z. X. Yang, L. Tang, G. M. Zeng, M. Yu, X. D. Li, H. P. Wu, Y. Y. Qian, X. M. Li, Y. Luo, Changes in heavy metal mobility and availability from contaminated wetland soil remediated with combined biochar-compost, Chemosphere 181 (2017) 281-288.

[36] A. P. de Mora, J. J. Ortega-Calvo, F. Cabrera, E. Madejón, Changes in enzyme activities and microbial biomass after "in situ" remediation of a heavy metal-contaminated soil, Appl. Soil Ecol. 28 (2005) 125-137.

[37] B. Maliszewska-Kordybach, B. Smreczak, Habitat function of agricultural soils as affected by heavy metals and polycyclic aromatic hydrocarbons contamination, Environ. Inter. 28 (2003) 719-728.

[38] S. Kang, M. S. Mauter, M. Elimelech, Microbial cytotoxicity of carbon-based nanomaterials: implications for river water and wastewater effluent, Environ. Sci. Technol. 43 (2009) 2648-2653.

[39] K. T. Kim, S. J. Klaine, S. Lin, P. C. Ke, S. D. Kim, Acute toxicity of a mixture of copper and single-walled carbon nanotubes to *Daphnia magna*, Environ. Toxicol. Chem. 29 (2010) 122-126.

[40] I. Kim, B. T. Lee, H. A. Kim, K. W. Kim, S. D. Kim, Y. S. Hwang, Citrate coated silver nanoparticles change heavy metal toxicities and bioaccumulation of *Daphnia magna*, Chemosphere 143 (2016) 99-105.

[41] F. Wang, J. Yao, H. Liu, R. Liu, H. Chen, Z. Yi, Q. Yu, L. Ma, B. Xing, Cu and Cr enhanced the effect of various carbon nanotubes on microbial communities in an

aquatic environment, J. Hazard. Mater. 292 (2015) 137-145.

[42] A. Nel, T. Xia, L. Mädler, N. Li, Toxic potential of materials at the nanolevel, Science 311 (2006) 622-627.

[43] O. Akhavan, E. Ghaderi, Toxicity of graphene and graphene oxide nanowalls against bacteria, ACS Nano 4 (2010) 5731-5736.

[44] H. Chung, Y. Son, T. K. Yoon, S. Kim, W. Kim, The effect of multi-walled carbon nanotubes on soil microbial activity, Ecotoxicol. Environ. Safety 74 (2011) 569-575.

[45] S. K. Manna, S. Sarkar, J. Barr, K. Wise, E. V. Barrera, O. Jejelowo, A. C. Rice-Ficht, G. T. Ramesh, Single-walled carbon nanotube induces oxidative stress and activates nuclear transcription factor-kB in human keratinocytes, Nano Lett. 5 (2005) 1676-1684.

[46] K. Kalbitz, S. Solinger, J. H. Park, B. Michalzik, E. Matzner, Controls on the dynamics of dissolved organic matter in soils: a review, Soil Sci. 165 (2000) 277-304.

[47] J. Martin, K. Haider, Microbial activity in relation to soil humus formation, Soil Sci. 111 (1971) 54-63.

[48] S. Yang, J. Hu, C. Chen, D. Shao, X. Wang, Mutual effects of Pb (II) and humic acid adsorption on multiwalled carbon nanotubes/polyacrylamide composites from aqueous solutions, Environ. Sci. Technol. 45 (2011) 3621-3627.

[49] F. Meng, G. Huang, X. Yang, Z. Li, J. Li, J. Cao, Z. Wang, L. Sun, Identifying the sources and fate of anthropogenically impacted dissolved organic matter (DOM)

in urbanized rivers, Water Res. 47 (2013) 5027-5039.

[50] C. A. Stedmon, D. N. Thomas, M. Granskog, H. Kaartokallio, S. Papadimitriou, H. Kuosa, Characteristics of dissolved organic matter in Baltic coastal sea ice: allochthonous or autochthonous origins? Environ. Sci. Technol. 41 (2007) 7273-7279.

[51] P. G. Coble, Characterization of marine and terrestrial DOM in seawater using excitation-emission matrix spectroscopy, Mar. Chem. 51 (1996) 325-346.

[52] N. Senesi, Molecular and quantitative aspects of the chemistry of fulvic acid and its interactions with metal ions and organic chemicals. Part II. The fluorescence spectroscopy approach, Anal. Chim. Acta 232 (1990) 77-106.

[53] X. Q. Lu, R. Jaffe, Interaction between Hg(II) and natural dissolved organic matter: a fluorescence spectroscopy based study, Water Res. 35 (2001) 1793-1803.

[54] F. Wu, Y. Cai, D. Evans, P. Dillon, Complexation between Hg(II) and dissolved organic matter in stream waters: an application of fluorescence spectroscopy, Biogeochemistry 71 (2004) 339-351.

[55] F. C. Wu, T. Midorikawa, E. Tanoue, Fluorescence properties of organic ligands for copper(II) in Lake Biwa and its rivers, Geochem. J. 35 (2001) 333-346.

[56] R. A. Saar, J. H. Weber, Comparison of spectrofluorometry and on-selective electrode potentiometry for determinations of complexes between fulvic acid and heavy-metal ions, Anal. Chem. 52 (1980) 2095-2100.

[57] Z. Wang, J. Cao, F. Meng, Interactions between protein-like and humic-like components in dissolved organic matter revealed by fluorescence quenching,

Water Res. 68 (2015) 404-413.

[58] J. Jaffrain, F. Gérard, M. Meyer, J. Ranger, Assessing the quality of dissolved organic matter in forest soils using ultraviolet absorption spectrophotometry, Soil Sci. Soc. Am. J. 71 (2007) 1851-1858.

[59] J. Peuravuori, K. Pihlaja, Molecular size distribution and spectroscopic properties of aquatic humic substances, *Anal. Chim. Acta*, 1997, 337, 133-149.

[60] K. Pandey, A study of chemical structure of soft and hardwood and wood polymers by FTIR spectroscopy, J. Appl. Polym. Sci. 71 (1999) 1969-1975.

[61] K. Pandey, A. Pitman, FTIR studies of the changes in wood chemistry following decay by brown-rot and white-rot fungi, Int. Biodeter. Biodegr. 52 (2003) 151-160.

[62] M. Amini, H. Younesi, N. Bahramifar, Biosorption of nickel (II) from aqueous solution by *Aspergillus niger*: response surface methodology and isotherm study, Chemosphere 75 (2009) 1483-1491.

[63] S. Amir, A. Jouraiphy, A. Meddich, M. El Gharous, P. Winterton, M. Hafidi, Structural study of humic acids during composting of activated sludge-green waste: elemental analysis, FTIR and ^{13}C NMR, J. Hazard. Mater. 177 (2010) 524-529.

[64] C. Jiang, G. R. Aiken, H. Hsu-Kim, Effects of natural organic matter properties on the dissolution kinetics of zinc oxide nanoparticles, Environ. Sci. Technol. 49 (2015) 11476-11484.

[65] A. J. Peters, J. Hamilton-Taylor, E. Tipping, Americium binding to humic acid, Environ. Sci. Technol. 35 (2001) 3495-3500.

[66] M. Schnitzer, Reactions between fulvic acid, a soil humic compound and inorganic

soil constituents, Soil Sci. Soc. Am. J. 33 (1969) 75-81.

[67] J. A. Leenheer, G. K. Brown, P. MacCarthy, S. E. Cabaniss, Models of metal binding structures in fulvic acid from the Suwannee River, Georgia, Environ. Sci. Technol. 32 (1998) 2410-2416.

[68] T. Lan, H. Wang, J. Liao, Y. Yang, Z. Chai, N. Liu and D. Wang, Dynamics of humic acid and its interaction with uranyl in the presence of hydrophobic surface implicated by molecular dynamics simulations, Environ. Sci. Technol. 50 (2016) 11121-11128.

[69] D.L. Huang, R. Deng, J. Wan, G.M. Zeng, W.J. Xue, X.F. Wen, C.Y. Zhou, L. Hu, X.G. Liu, X.Y. Guo, X.Y. Ren. Remediation of lead-contaminated sediment by biochar-supported nano-chlorapatite: Accompanied with the change of available phosphorus and organic matters. J. Hazard. Mater. 348 (2018) 109-116.

Figure lengends

Fig. 1. TEM images of pristine MWCNTs at day 0 (a); TEM images of MWCNTs-sediment mixture after 90 days of incubation (b, c). Nitrogen adsorption–desorption isotherms and pore size distributions (insets) of MWCNTs (d); XPS survey spectra (e), high-resolution spectra for C1s (f) and O1s (g) MWCNTs at day 0 and 90.

Fig. 2. Dynamic Cd sink and TCLP extracted Cd contents variation in the Cd and MWCNTs incorporation sediments during 90 days of incubation. Different letters indicate significant differences ($p < 0.05$).

Fig. 3. Response of urease activity to MWCNTs and Cd-MWCNTs co-incorporation at day 10 (a) and 30 (b). Different letters indicate significant differences ($p < 0.05$).

Fig. 4. Variation of humic substances (HS), fulvic acids (FA) and humic acids (HA) during 90 days of incubation. Different letters indicate significant differences ($p < 0.05$).

Fig. 5. Excitation-emission matrices (EEMs) spectra of FA and HA for selected samples at day 60.

Fig. 6. Spectroscopic indices for aromaticity (A_{280}, E_2/E_3, $f_{450/500}$), for humification (A_{254}) and for hydrophobicity (A_{260}) of FA fraction at day 10 (a) and day 60 (b).

Fig. 7. FTIR spectra of HA for selected samples at day 10 (a) and day 60 (b).

Fig. 8. Variation of Cd contents complexed by extracted humic substances and mass ratios of Cd contents complexed by extracted humic substances. (** represents the significant differences ($p<0.01$)).

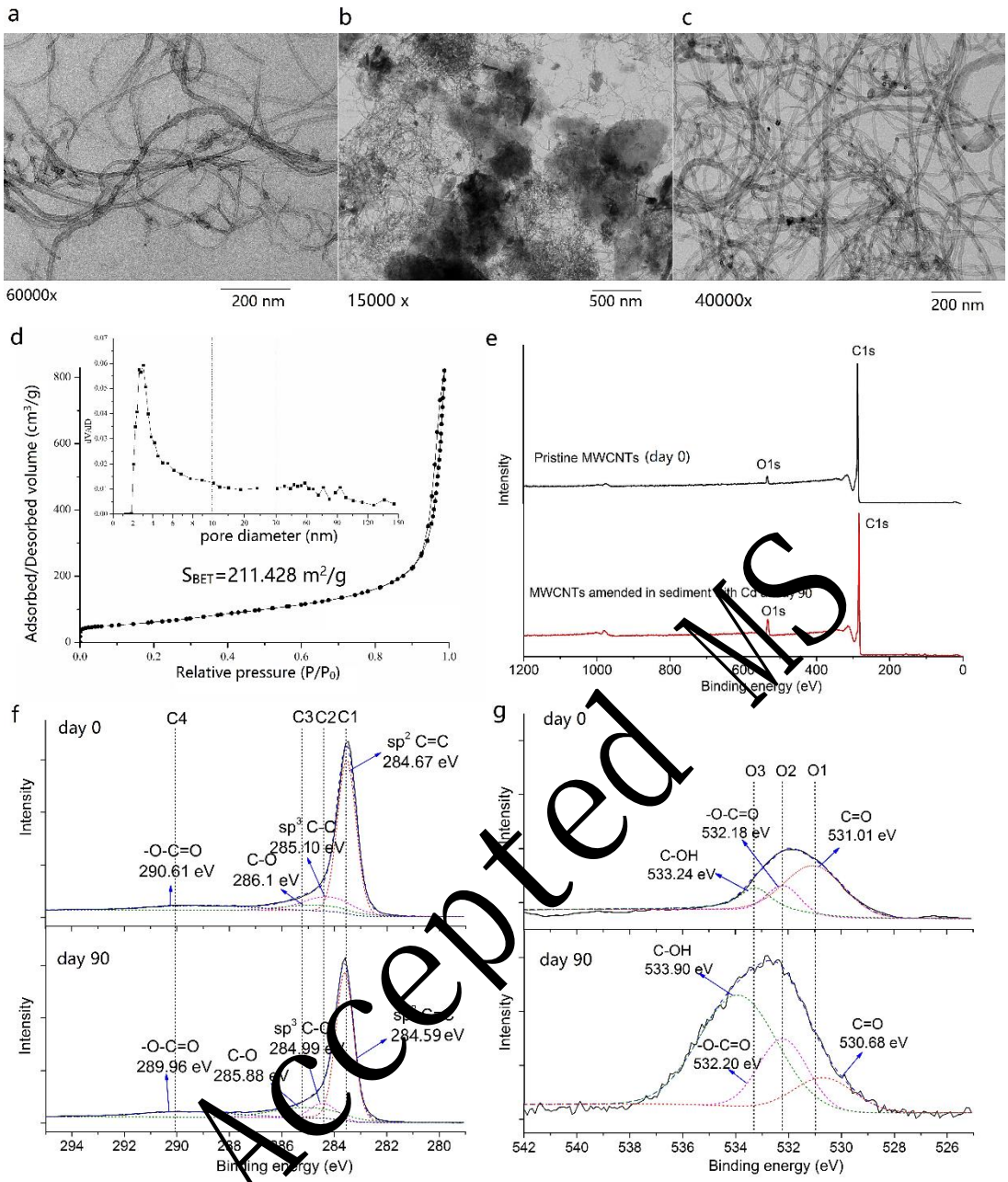

Fig. 1.

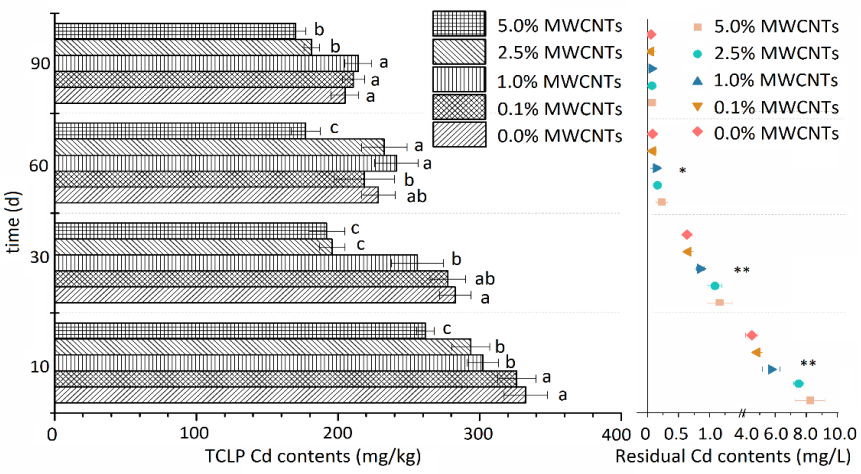

Fig. 2.

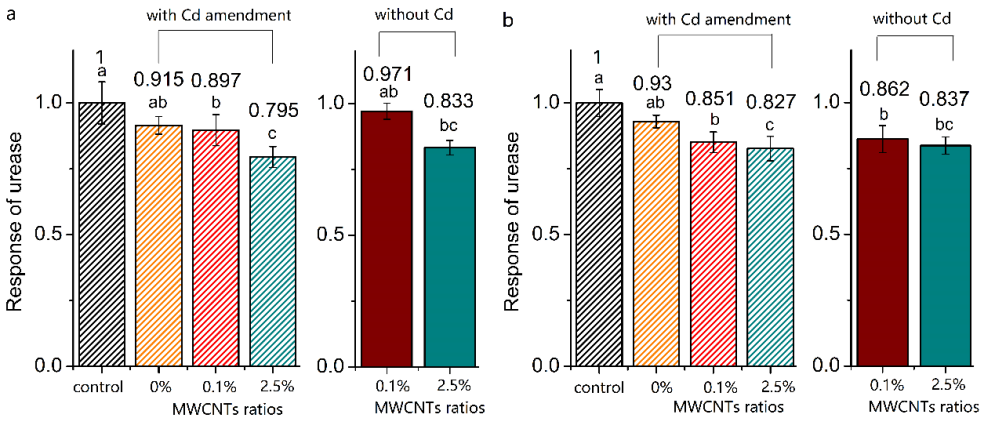

Fig. 3.

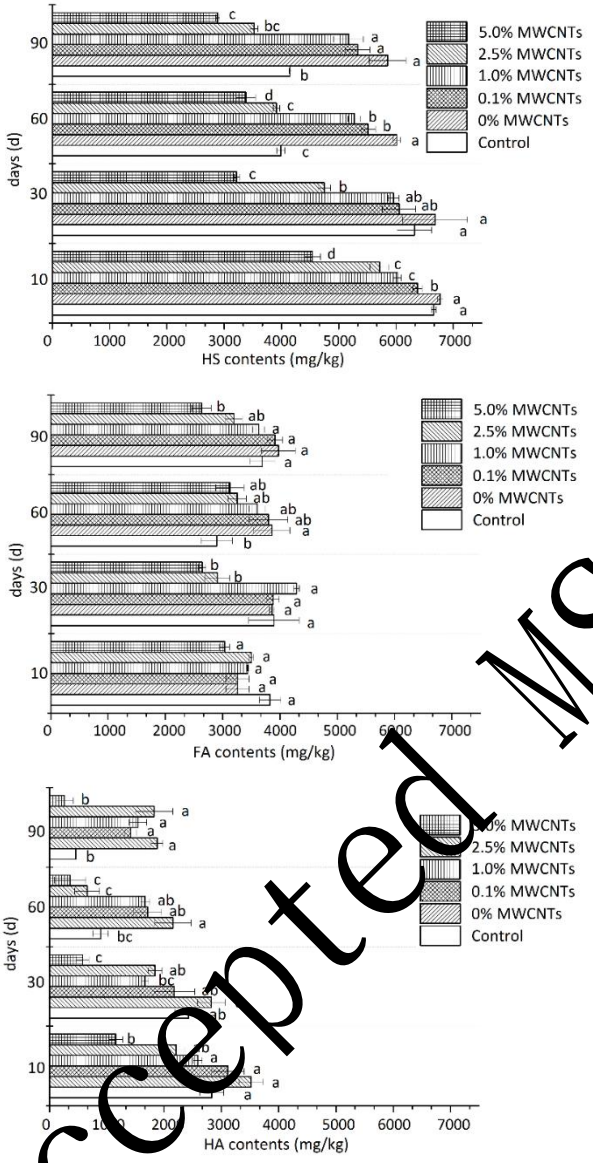

Fig. 4.

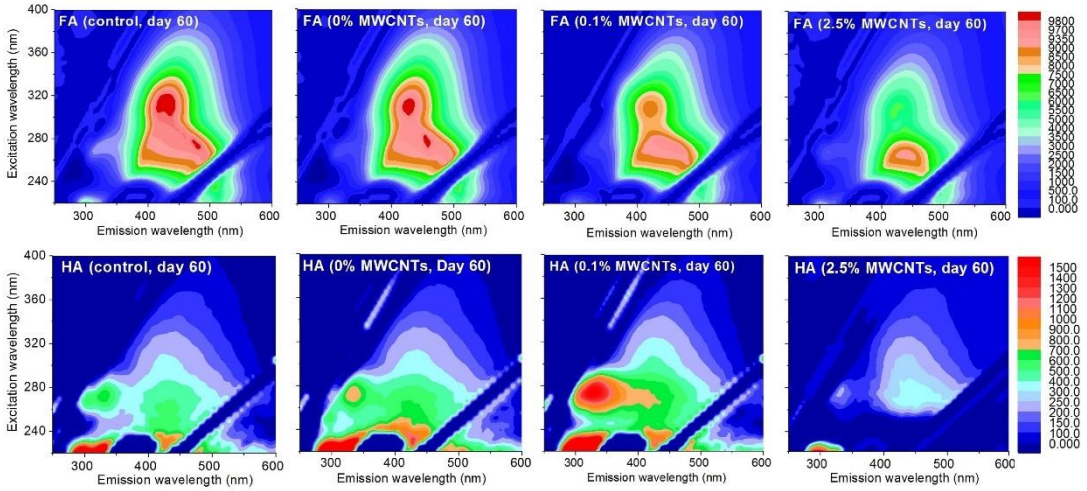

Fig. 5.

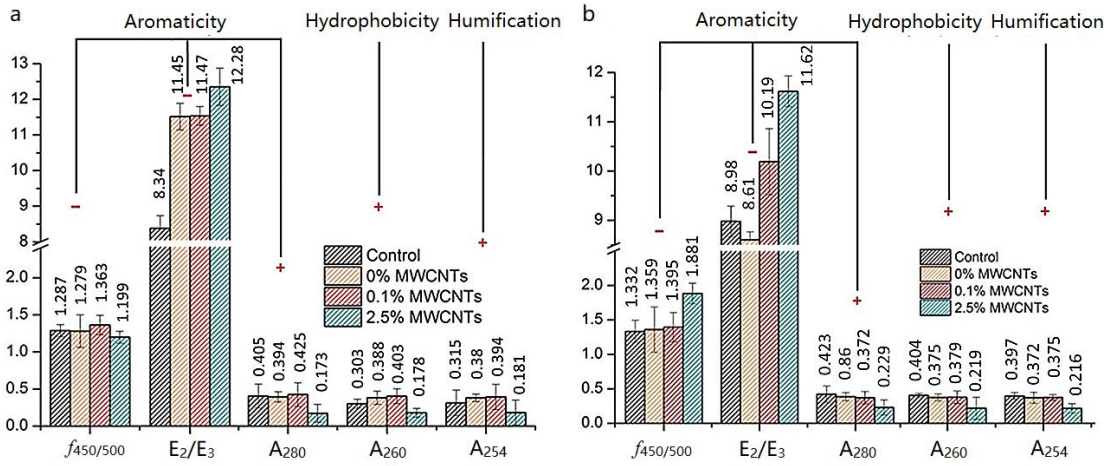

Fig. 6.

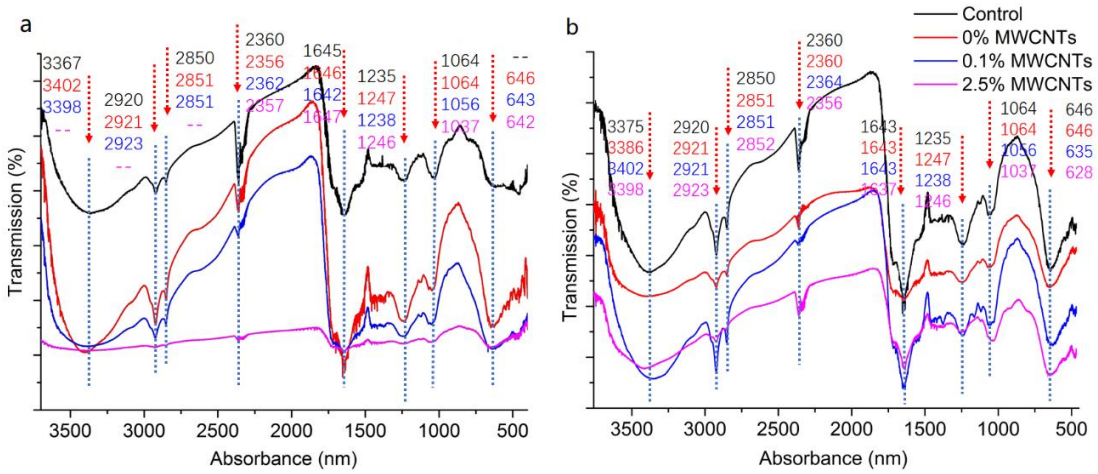

Fig. 7.

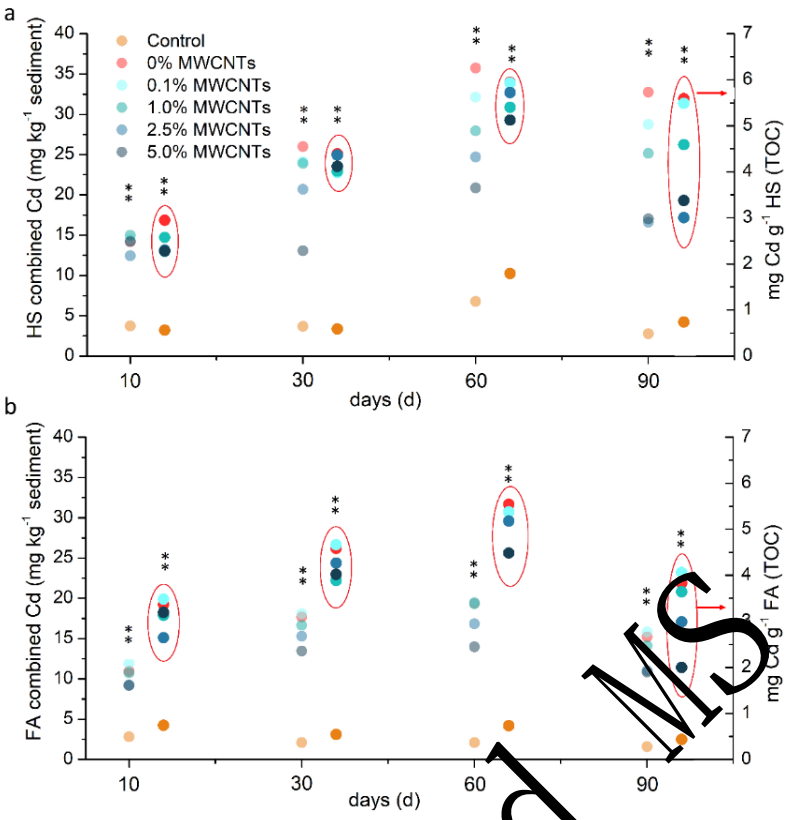

Fig. 8.